Effective Temperature in Stochastic Kinetics and Gene Networks

Ting Lu,*§ Jeff Hasty,† and Peter G. Wolynes*‡§
*Department of Physics, †Department of Bioengineering, ‡Department of Chemistry and Biochemistry, and §Center for Theoretical Biological Physics, University of California, San Diego, La Jolla, California 92093-0371

ABSTRACT   The fluctuation-dissipation theorem, one of the central theorems in thermal dynamics, breaks down in out-of-equilibrium systems. The idea of effective temperature coming from the extensions of that theorem has been recently introduced to study glasses and has proved to be a key concept for out-of-equilibrium systems. Gene networks involve stochastic chemical kinetics and are far from equilibrium. This leads us to try to use the notion of effective temperature to study them. To develop this idea, we study a simple birth-death process and a general two-species interacting process using the language of effective temperature. Furthermore, a model of a nonregulatory gene is studied as an example. The effective temperature may serves as an alternative and somewhat more fundamental language to describe the intrinsic-extrinsic noise distinction that has already provided a tool for qualifying gene networks.

INTRODUCTION

Gene networks are inherently noisy systems, with fluctuations arising from the stochastic nature of the underlying biochemical reaction events (1–3). Fluctuations become more important when the numbers of reactant molecules are small, as is often the case in gene regulatory networks. The role of noise in gene expression has attracted much attention over the past few years, and many approaches have been used to model these systems. The Gillespie algorithm (4–6) is often considered to be the gold standard for performing stochastic simulations of such stochastic biological processes.

The noise in gene networks can been classified as either intrinsic, related to the specific biochemical process under evaluation, or extrinsic, related to factors upstream of this process (7,8). Various groups have experimentally investigated the effect that each source has on gene expression, and these studies have greatly improved our understanding of stochastic gene networks. Recent articles have laid a foundation for comparing experimental data with quantitative models of simplified gene networks (9,10) and have shown that noise may limit the sensitivity of gene networks (11).

Many such models have employed the fluctuation-dissipation theorem, the central theorem in equilibrium mechanics, to describe these networks (12). However, gene networks are complex, far-from-equilibrium systems for which the fluctuation-dissipation theorem may break down. In this article, we explore how the fluctuation-dissipation theorem may apply or break down in the realm of stochastic biochemical processes.

One of the key topics in quantitative biology is the search for measurable quantities that can be used to characterize the properties of a gene network. Here we explore the potential that effective temperature may provide such a quantitative measure. In thermodynamics, temperature must be same for two bodies when they are in thermal equilibrium (13). At equilibrium, temperature is independent of which part of a system and the precise measurements made. Near equilibrium, temperature differences determine the direction of heat flow. When a system is far from equilibrium, these key principles of thermodynamics may fail. Nevertheless, it has been possible to extend the concept of temperature in thermodynamics to effective temperature in nonequilibrium systems (14) that change sufficiently slowly, such as glassy systems (15,16).

Since genetic systems often respond much more slowly than the rate of their individual reaction events, we are encouraged to examine whether effective temperature plays an important role in gene networks. In fact, a few studies have already employed effective temperature to investigate biological systems. For example, it has been used to study the stability of motorized particles in cytoplasm (17) and to reveal the underlying active process in hair bundles (18). Here we examine effective temperature as determined by comparing fluctuation to response in stochastic kinetics with the application to gene networks in mind. Our first example focuses on the effective temperature of a simple birth-death process. We then generalize our argument to describe the kinetics of two-species interactions.

The article is organized as follows. After introducing the definition of effective temperature, we investigate a birth-death process where exact expressions for the effective temperature are derived both in the cases where there are large and small numbers of particles. Monte Carlo simulations are compared to these exact results. We then study a general system of two interacting chemical species. For this system, analytical results are derived using Langevin method relevant for a relatively large numbers of particles. For the two species problem we can examine whether temperature

gradients determine the direction of flows. Finally, we use the effective temperature to study an unregulated gene where both intrinsic and extrinsic noise is quantified using effective temperature. We conclude with a general discussion.

EFFECTIVE TEMPERATURE

Let us start with a classical exercise that interested Einstein 1 century ago (12,19). In the presence of a given potential field $V(x)$, particles flow with the drift velocity $J_F = -\mu c(\partial V(x)/\partial x)$, where μ is the mobility and c is the concentration of particles at the position x. On the other hand, particles diffuse randomly and obey the Ficks first law of diffusion as $J_D = -D(\partial c/\partial x)$. In thermal equilibrium, particles are in the Boltzmann distribution, i.e., $c \sim exp[-V(x)/k_B T]$, and the net current $J_N = J_F - J_D$ is null, i.e., $-\mu c(\partial V(x)/\partial x) + D(\partial c/\partial x) = 0$. Therefore the mobility, due to the friction of particles, and the diffusion, due to the random motions of the particles, are directly related:

$$\mu = \frac{1}{k_B T} D. \qquad (1)$$

This has become known as the Einstein relation. This relation between fluctuation (D) and response (μ), when manifested in a more general manner, is called fluctuation-dissipation theorem.

The fluctuation-dissipation theorem states a general relationship between the response of a given system to an external disturbance and the internal fluctuations of the system in equilibrium. This relationship contains the temperature and is central in thermodynamics. However, when a system is out of equilibrium, the theorem breaks down and an extension of the theorem must be made. So the concept of effective temperature is introduced.

In a near equilibrium system, it is customary to study mechanical fluctuations and response. Consider such a mechanical system with a Hamiltonian H. If O_1 and O_2 are two observables of the system, then the correlation between these two observables is described by the function

$$C_{12}(t',t) = \langle O_1(t')O_2(t)\rangle - \langle O_1(t')\rangle\langle O_2(t)\rangle, \qquad (2)$$

where the brackets indicate the ensemble average.

If the system is subjected to a time-dependent small perturbation $-h(t)O_2(t)$, where $h(t)$ is a small field and $O_2(t)$ is an observable, then the Hamiltonian becomes

$$H \rightarrow H - h(t)O_2(t). \qquad (3)$$

The response of the average of the observable O_1 to the small perturbation $-h(t)O_2(t)$ is then given by

$$R_{12}(t',t) = \frac{\delta\langle O_2(t')\rangle}{\delta h(t)}. \qquad (4)$$

For systems with slow dynamics, Cugliandolo et al. (15) suggests the effective temperature in the Fourier space may be defined as

$$T_{\text{eff}}(\omega) \equiv \frac{\omega \tilde{C}'_{12}(\omega)}{\tilde{R}''_{12}(\omega)}, \qquad (5)$$

where $\tilde{C}'_{12}(\omega)$ is the real part of the Fourier transform of the correlation function Eq. 2 and $\tilde{R}''_o(\omega)$ is the imaginary part of the Fourier transform of the response Eq. 4, i.e., $\tilde{C}'_{12}(\omega) = \mathcal{I}\{\int_0^\infty dt C_{12}(t)e^{i\omega t}\}$, $\tilde{R}''_{12}(\omega) = \mathcal{R}\{\int_0^\infty dt R_{12}(t)e^{i\omega t}\}$.

Genetic networks are generally multi-timescale systems. The characteristic time of binding events is much shorter than the half-life of the messenger RNA, which in turn is one order of magnitude shorter than the half-life of the resulting protein. Cell-to-cell communications and transportation processes are even possibly slower. These multiple scale properties encourage us to investigate the role of defining effective temperatures in genetic networks.

A BIRTH-DEATH PROCESS

Genetic networks are extremely complex, involving binding processes, synthesis processes, and degradation processes. To understand the fundamental properties of noise in gene networks, the response of networks to small perturbations, and the effective temperatures, we begin with the simplest birth-death process, which describes synthesis and degradation. Studying the simple birth-death process already helps us understand the limits of the effective temperature concept. The reactions of a simple birth-death process are shown in Table 1. The master equation for this process reads

$$\frac{\partial}{\partial t}P(x,t) = g(x-1)P(x-1,t) - g(x)P(x,t)$$
$$+ d(x+1)P(x+1,t) - d(x)P(x,t). \qquad (6)$$

Large *N* case

When the numbers of particles are large, the master equation can be approximated by the Fokker-Planck equation, which is equivalent to the Langevin equation:

$$\frac{d}{dt}x = g(x) - d(x) + \eta(t), \qquad (7)$$

where $\eta(t)$ is a Gaussian white noise term, i.e., $\langle\eta(t)\rangle = 0$, $\langle\eta(t)\eta(t')\rangle = [g(x) + d(x)]\delta(t - t')$. Comparing this simple birth-death process with the Brownian motion of an over-

TABLE 1   Birth-death process

Reaction	Rate	Specified rate
$\phi \rightarrow X$	$g(x)$	k_g
$X \rightarrow \phi$	$d(x)$	k_d

damped particle (20), we have the effective temperature of this process:

$$T_{eff} = \frac{1}{2}\{g(x) + d(x)\}, \qquad (8)$$

where T_{eff} can be further simplified as $T_{eff} = g(x)$ if the system is near the steady state where $g(x) - d(x) = 0$ holds. If we specify $g(x)$ and $d(x)$ as those listed in the third column of Table 1, the effective temperature becomes $T_{eff} = k_g$.

The effective temperature of this birth-death process can also be derived from the effective fluctuation-dissipation (FD) relationship. There are two kinds of perturbations that can be used to calculate effective temperature according to the FD relation. We may use a perturbation of generation rate k_g or a perturbation of degradation rate k_d. Both of these perturbations yield the same effective temperature $T_{eff} = k_g$. This result is consistent with Eq. 8, which verifies the validity of the definition of effective temperature in the large N limit.

Small *N* case

In the last subsection, Eq. 7 is appropriate for large number limit. But we also wish to define the effective temperatures in the small number case to see if they the same. To answer these questions, we first use the operator formulism for master equations (21) combined with Eyink's variational method (22) to get the correlation and response and thus the effective temperatures for any value of the mean number.

In the operator formulation, the master equation Eq. 6 with specified reaction rates is written as

$$\frac{d}{dt}|\Psi(t)\rangle = \hat{L}|\Psi(t)\rangle, \qquad (9)$$

where the Liouvillian is $\hat{L} = k_g(\hat{a}^+ - 1) + k_d(\hat{a} - \hat{a}^+\hat{a})$. The Liouvillian is generally non-Hermitian, i.e., $\hat{L} \neq \hat{L}^+$. The state function $|\Psi(t)\rangle$ is defined as $|\Psi(t)\rangle \equiv \sum_0^\infty P(n,t)|n\rangle$, where $P(n, t)$ is the probability of having n number of X at time t and $|n\rangle$ is the state with n number of X. $\hat{a}$ and $\hat{a}^+$ are creation and annihilation operators, respectively, which have the relations $\hat{a}|n\rangle = n|n-1\rangle$, $\hat{a}^+|n\rangle = |n+1\rangle$ and $[\hat{a}, \hat{a}^+] = 1$.

To solve Eq. 9, we use the coherent trial Ansätze $\langle\Psi^L| = \langle 0|e^{\hat{a}}(1+\alpha(\hat{a}^+\hat{a} - 1))$ and $|\Psi^R\rangle = e^{u(\hat{a}^+ - 1)}|0\rangle$. The action for the system is

$$\Gamma = \int_0^\infty dt \langle\Psi^L(t)|(\partial_t - \hat{L})|\Psi^R(t)\rangle. \qquad (10)$$

The variations of the action generate two equations for the parameters α and u:

$$\frac{d}{dt}\alpha(t) = -k_d\alpha(t) \qquad (11)$$

$$\frac{d}{dt}u(t) = k_g - k_d u(t). \qquad (12)$$

The steady states of the system $\langle\Psi_s^L| = \langle 0|e^{\hat{a}}$ and $|\Psi_s^R\rangle = e^{u_s(\hat{a}^+ - 1)}|0\rangle$ are then found by taking $\alpha = 0$ and $u = k_g/k_d \equiv u_s$ in the above equations. This indicates that the steady-state distribution is a Poisson distribution with the mean u_s. This is confirmed to be the exact distribution by solving the master equation using the generating function method (23). The operator formulation, although cumbersome for the distribution function, is advantageous for calculating correlation and response functions, as we see in the following description.

Recall that there are two types of perturbations of the system—a perturbation of generation rate and a perturbation of degradation rate. These correspond to the perturbations of the Liouvillian $\hat{L}$ by $-h(t)(\hat{a}^+ - 1)$ and $-h(t)(\hat{a} - \hat{a}^+\hat{a})$. Because the Liouvillian is non-Hermitian ($\hat{L} \neq \hat{L}^+$), the left and state functions are not conjugate, i.e., $|\Psi^R(t)\rangle \neq (\langle\Psi^L(t)|)^+$. Likewise the time-dependent expression for an operator in the Heisenberg representation of the stochastic process is somewhat different from that for quantum system with a Hermitian Hamiltonians.

In the non-Hermitian case, a time-dependent operator can be defined as (24)

$$\hat{A}(t) = \hat{\bar{U}} + \hat{A}_s\hat{U}, \qquad (13)$$

where $\hat{U}$ and $\hat{\bar{U}}^+$ are the evolution operators for the forward and backward Kolmogorov processes, respectively. Because of the non-Hermitian property of the Liouvillian, the forward evolution operator is not the $\hat{\bar{U}}$ conjugate of the backward, i.e., $(\hat{U})^+ \neq \hat{\bar{U}}^+$. However, $\hat{U}$ and $\hat{\bar{U}}^+$ should conserve the evolution, i.e., $\hat{\bar{U}}^+\hat{U} = \hat{U}\hat{\bar{U}}^+ = 1$.

Now we turn to the calculation of correlation and response functions. For a perturbation of Liouvillian corresponding to the generation rate with $\hat{L} - h(t)(\hat{a}^+ - 1)$, the corresponding correlation and response functions can be obtained after some algebra (see Appendix A). These are

$$C(t',t) = u_s^2 + u_s e^{-k_d(t'-t)} \qquad (14)$$

$$R(t',t) = e^{-k_d(t'-t)} \qquad (15)$$

from which the effective temperature may be derived:

$$T_{eff}^g = k_g. \qquad (16)$$

This is exactly the same as what was obtained in the large number limit.

On the other hand, for a perturbation of the degradation rate of the Liouvillian with $\hat{L} - h(t)(\hat{a} - \hat{a}^+\hat{a})$, the corresponding correlation and response functions (see Appendix A) are

$$C(t',t) = \frac{1}{2}\left(u_s^3 + u_s^2 + 2u_s^2 e^{-k_d(t'-t)} + u_s e^{-k_d(t'-t)}\right) \qquad (17)$$

$$R(t',t) = u_s e^{-k_d(t'-t)}. \qquad (18)$$

The effective temperature is thus found to be

$$T_{eff}^d = k_g + k_d/2. \qquad (19)$$

This temperature is different from either the one found by perturbing the generation rate in small number regime Eq. 16 or what was found in large number limit Eq. 8.

For this birth-death process, the percentage of the relative difference of the two temperatures is $50k_{\mathrm{d}}/k_{\mathrm{g}}\%$. When the average number of a protein $k_{\mathrm{g}}/k_{\mathrm{d}}$ is 10, the difference of the two temperatures is 5%, which is already obvious. Further, when the average number is ~ 1, the difference will be up to 50%. In some natural and synthetic genetic systems, the numbers of molecules are actually small. One study shows that the freely available dimers of the repressors CI in the phage λ are only ~ 10 (25,26), in which case small number will be an important effect. This effect might be dominant in those cases where there are few copies or even sometimes a single copy of a gene in the natural genome or in the case of there being only a few copies of plasmids in a cell.

However, when the number of molecules is large, i.e., $k_{\mathrm{g}}/k_{\mathrm{d}} \gg 1$, both $T_{\mathrm{eff}}^{\mathrm{g}}$ and $T_{\mathrm{eff}}^{\mathrm{d}}$ merge consistently to the large number limiting value k_{g}.

Comparison with simulations

To check the effective temperatures derived analytically, we carried out some explicit simulations. We used the Gillespie simulation (4) to generate data following the reaction rules in Table 1. We use the rate coefficients shown in the Table 1 to generate data for each run and made 10,000 runs of the program to represent the ensemble of trajectories. We numerically calculated the correlations and use averaged response.

To calculate the response function, we actually found the frequency-dependent susceptibility of the system rather than response function just as one would do in real experiments (15). The simulation first ''equilibrated'' after waiting for a long enough time to allow the system comes to a steady state and to fluctuate around that state. We then turned on the perturbations (for a perturbation of generation rate, we use $k_{\mathrm{g}}' = k_{\mathrm{g}}(1 + 5\%)$; for a perturbation of degradation rate, we use $k_{\mathrm{d}}' = k_{\mathrm{d}}(1 + 5\%)$). We recorded all of the data once the perturbation was added; 10,000 independent runs provided an ensemble that could be numerically averaged to get the susceptibility.

Following Cugliandolo and Kurchan, we can draw parametric fluctuation-dissipation plots of the response versus the correlation, where the negative reciprocal of the slope of the curve indicates the effective temperature (15). Fig. 1 clearly indicates that for a perturbation of $-h(t)(\hat{a}^{+} - 1)$, the slope is always equal to $-1/k_{\mathrm{g}}$. This result is found regardless of the mean values of the species number. This means that the corresponding effective temperature is always k_{g}. However, we can see from Fig. 2 that for a perturbation of $-h(t)(\hat{a} - \hat{a}^{+}\hat{a})$, the slope of the simulation is equal to $-1/(k_{\mathrm{g}} + k_{\mathrm{d}}/2)$. This difference becomes clearer when the mean number is small in panel D. For this observable, we see that the corresponding effective temperature is $k_{\mathrm{g}} + k_{\mathrm{d}}/2$ rather than
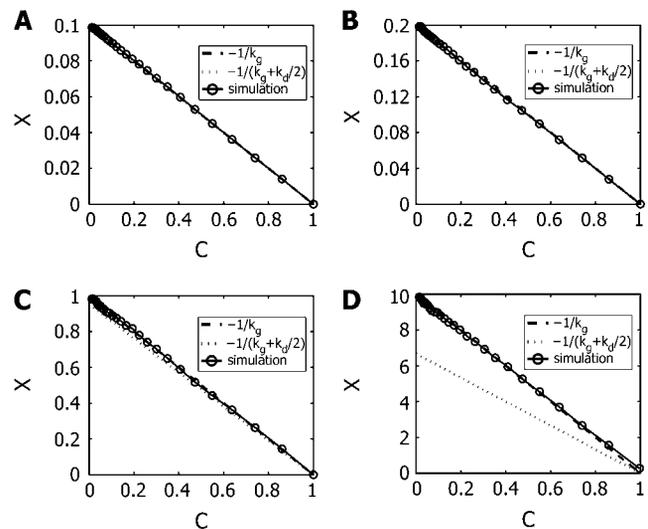

FIGURE 1 Effective temperatures corresponding to different mean value numbers $k_{\mathrm{g}}/k_{\mathrm{d}}$ for a perturbation of $-h(t)x$. The parameters $\{k_{\mathrm{g}} = 10.0, k_{\mathrm{d}} = 0.1\}$, $\{k_{\mathrm{g}} = 5.0, k_{\mathrm{d}} = 0.1\}$, $\{k_{\mathrm{g}} = 1.0, k_{\mathrm{d}} = 0.1\}$ and $\{k_{\mathrm{g}} = 0.1, k_{\mathrm{d}} = 0.1\}$ are chosen in panels A, B, C, and D, respectively. Dashed lines have a slope of $-1/k_{\mathrm{g}}$, dotted lines have a slope of $-\nu 1/k_{\mathrm{g}} + k_{\mathrm{d}}/2$, and lines with circles are the simulation results with corresponding reaction rates. The x and y axes are correlation and susceptibility, respectively, and both are scaled so that the correlations range from 0 to 1 in all of the figures for comparison.

k_{g}. Although these two effective temperatures are not the same, they tend to become equal when the mean number becomes large (e.g., the *left upper panels* in Figs. 1 and 2). Both of the simulations agree very well with the analytical results in the above subsection.
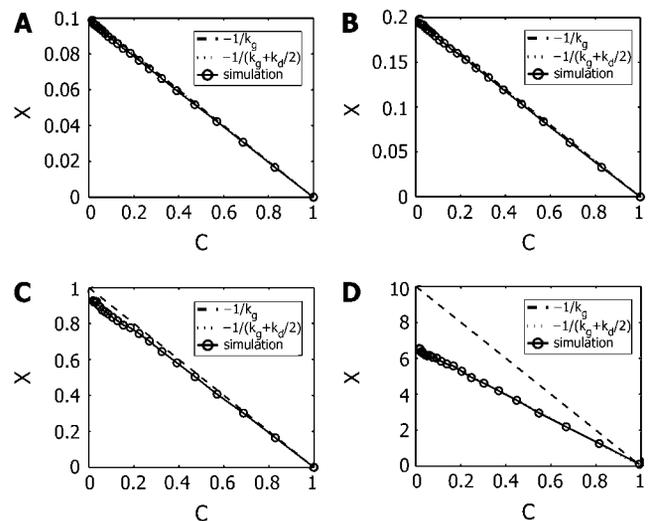

FIGURE 2 Effective temperatures corresponding to different mean value numbers $k_{\mathrm{g}}/k_{\mathrm{d}}$ for the perturbations of $-h(t)x^2$. The parameters $\{k_{\mathrm{g}} = 10.0, k_{\mathrm{d}} = 0.1\}$, $\{k_{\mathrm{g}} = 5.0, k_{\mathrm{d}} = 0.1\}$, $\{k_{\mathrm{g}} = 1.0, k_{\mathrm{d}} = 0.1\}$ and $\{k_{\mathrm{g}} = 0.1, k_{\mathrm{d}} = 0.1\}$ are chosen in panels A, B, C, and D, respectively. Dashed lines have a slope of $-1/k_{\mathrm{g}}$, dotted lines have a slope of $-\nu 1 k_{\mathrm{g}} + k_{\mathrm{d}}/2$, and lines with circles are the simulation results with corresponding reaction rates. The x and y axes are correlation and susceptibility, respectively; both are scaled so that the correlations range from 0 to 1 in all of the figures for comparison.

Physical interpretation

Both the analytical and numerical results show that there is more than one effective temperature for a birth-death process. Effective temperature is thus not a unique quantity, but rather is observable-dependent. This result is surprising given the general properties of effective temperature for a far-from-equilibrium system (14). In equilibrium systems, all of the effective temperatures must converge to the same value regardless of the observable used in measurements (12), but this need not be the case for an out-of-equilibrium system. The fact that there are two different effective temperatures does not contradict our physical intuition, but simply emphasizes that the system in a steady state is not a true state of equilibrium.

The two effective temperatures explore different aspects of the system dynamics in the steady states corresponding to two different perturbations. The difference between the two temperatures is, however, a ''higher order'' correction in some sense. As shown above, they converge to each other in the large number limit.

A TWO-SPECIES INTERACTING PROCESS

Now we turn to a more complex example involving interactions between two species. The two species A and B may have their own generation and degradation processes, and if one species is consumed by the other, they become correlated due to this interaction (Table 2). When their numbers are high, the two species essentially interact as a predator-prey system and may be described by Langevin equations: (28)

$$\frac{\partial}{\partial t}A = k_{g1} - d_1 A + f_2 B + D_1 \xi_1(t) + D_3^a \xi_3(t) + D_4^a \xi_4(t) \quad (20)$$

$$\frac{\partial}{\partial t}B = k_{g2} - d_2 B + f_1 A + D_2 \xi_2(t) + D_3^b \xi_3(t) + D_4^b \xi_4(t), \quad (21)$$

where $d_1 = k_{d1} + (1 - m_1)u$, $d_2 = k_{d2} + (1 - m_2)v$, $f_1 = n_1 u$, and $f_2 = n_2 v$. $\xi_i(t)$ is a Gaussian normal noise with the properties $\langle \xi_i(t) \rangle = 0$ and $\langle \xi_i(t)\xi_j(t') \rangle = \delta_{i,j} \cdot \delta(t - t')$. Their noise intensities are $D_1 = \sqrt{k_{g1}+k_{d1}A}$, $D_2 = \sqrt{k_{g2}+k_{d2}B}$, $D_3^a = (m_1 - 1)\sqrt{uA}$, $D_3^b = n_1\sqrt{uA}$, $D_4^a = n_2\sqrt{vB}$, and $D_4^b = (m_2 - 1)\sqrt{vB}$.

The correlations arising from the interactions enter as common noise terms in Eqs. 20 and 21. These linear equations could arise from a nonlinear system by linearizing around the

TABLE 2 Two-species interacting process

Reaction	Rate constant
$\phi \rightarrow A$	k_{g1}
$A \rightarrow \phi$	k_{d1}
$\phi \rightarrow B$	k_{g2}
$B \rightarrow \phi$	k_{d2}
$A \rightarrow m_1 A + n_1 B$	u
$B \rightarrow m_2 B + n_2 A$	v

steady states. This is especially relevant in the current context, since both the correlations and response are only calculated when the system is at a steady state. The numbers m_1, m_2, n_1, and n_2 can be arbitrary positive or negative integers, and represent different types of interactions between the two species. For example, $m_1 = m_2 = 1$, $n_1 = n_2 = -1$ implies that A consumes B and there is competition between A and B, whereas $m_1 = m_2 = 0$, $n_1 = n_2 = 1$ means A reacts to B and B reacts to A. All of the reaction rates are shown in column two of Table 2. We note that for a system of molecular species, the steady-state values should be positive, i.e.,

$$A^* = \frac{f_2 k_{g2} + d_2 k_{g1}}{d_1 d_2 - f_1 f_2} > 0 \quad (22)$$

$$B^* = \frac{f_1 k_{g1} + d_1 k_{g2}}{d_1 d_2 - f_1 f_2} > 0 \quad (23)$$

$$d_1 d_2 - f_1 f_2 \neq 0. \quad (24)$$

Effective temperature of the two-species system

As explored in the single birth-death process, generally there are multiple effective temperatures, with different temperatures corresponding to measurements using different perturbations. Instead of comparing all of the temperatures of the two species, we focus on the effective temperature corresponding to the perturbation of the generation rates and the autocorrelation of one species as a measurement for the interacting process. Other effective temperatures can be derived in straightforward fashion. We will lose some information by using only one of the effective temperatures corresponding to the autocorrelation, but we will still capture the essence of the situation.

The autocorrelations of A and B for the two interacting species are derived using the Fourier transform (see Appendix B)

$$C_{AA} = \frac{(\omega^2 + d_2^2)D_1^2 + f_2^2 D_2^2 + [(d_2 D_3^a + f_2 D_3^b)^2 + \omega^2 (D_3^a)^2] + [(d_2 D_4^a + f_2 D_4^b)^2 + \omega^2 (D_4^a)^2]}{(\omega^2 + f_1 f_2 - d_1 d_2)^2 + (d_1 + d_2)^2 \omega^2} \quad (25)$$

$$C_{BB} = \frac{f_1^2 D_1^2 + (\omega^2 + d_1^2)D_2^2 + [(f_1 D_3^a + d_1 D_3^b)^2 + \omega^2 (D_3^b)^2] + [(f_1 D_4^a + d_1 D_4^b)^2 + \omega^2 (D_4^b)^2]}{(\omega^2 + f_1 f_2 - d_1 d_2)^2 + (d_1 + d_2)^2 \omega^2}. \quad (26)$$

The response functions can be derived similarly (see Appendix B):

$$R_{AA} = \frac{i\omega - d_2}{\omega^2 + i\omega(d_1 + d_2) + f_1 f_2 - d_1 d_2} \qquad (27)$$

$$R_{BB} = \frac{i\omega - d_1}{\omega^2 + i\omega(d_1 + d_2) + f_1 f_2 - d_1 d_2}. \qquad (28)$$

Following the definition Eq. 5, we have the effective temperature for species A and B from Eqs. 25–28:

$$T_{eff}^{AA}(\omega) = \frac{(\omega^2 + d_2^2)D_1^2 + f_2^2 D_2^2 + [(d_2 D_3^a + f_2 D_3^b)^2 + \omega^2 (D_3^a)^2] + [(d_2 D_4^a + f_2 D_4^b)^2 + \omega^2 (D_4^a)^2]}{\omega^2 + f_1 f_2 + d_2^2} \qquad (29)$$

$$T_{eff}^{BB}(\omega) = \frac{f_1^2 D_1^2 + (\omega^2 + d_1^2)D_2^2 + [(f_1 D_3^a + d_1 D_3^b)^2 + \omega^2 (D_3^b)^2] + [(f_1 D_4^a + d_1 D_4^b)^2 + \omega^2 (D_4^b)^2]}{\omega^2 + f_1 f_2 + d_1^2}. \qquad (30)$$

These are the effective temperatures of the predator-prey system. The expressions show that the effective temperature for each species depends not only on its own birth-death rate but also on the birth-death rate of the other species. They are correlated by interacting terms.

The temperatures depend on the timescale just as they do for other nonequilibrium systems, e.g., glasses (15), where the fluctuation-dissipation theorem in its simple form breaks down (12). A convenient way to illustrate this breaking down is to draw correlation-susceptibility plots (15), since the negative reciprocal of the slope of the curves indicates the effective temperature of a system. For the simplicity, we set the birth-death noise terms D_1 and D_2 to be constants, and set the correlated noise terms D_3^a, D_3^b, D_4^a, and D_4^b to be zero. This is a simplified version of the general interacting process shown above. However, even this simple system suffices to demonstrate the breaking down of the fluctuation-dissipation relation. Here we employ the inverse Fourier transform to get the correlation and response functions in real space and then draw the plots.

$$C_{AA}(t) = \frac{[d_2^2 - (x-y)^2]T_1 + f_2^2 T_2}{4xy(x-y)}e^{-(x-y)t}$$
$$- \frac{[d_2^2 - (x+y)^2]T_1 + f_2^2 T_2}{4xy(x+y)}e^{-(x+y)t} \qquad (31)$$

$$C_{BB}(t) = \frac{[d_1^2 - (x-y)^2]T_2 + f_1^2 T_1}{4xy(x-y)}e^{-(x-y)t}$$
$$- \frac{[d_1^2 - (x+y)^2]T_2 + f_1^2 T_2}{4xy(x+y)}e^{-(x+y)t} \qquad (32)$$

$$R_{AA}(t) = \frac{(x+y) - d_2}{2y}e^{-(x+y)t} - \frac{(x-y) - d_2}{2y}e^{-(x-y)t} \qquad (33)$$

$$R_{BB}(t) = \frac{(x+y) - d_2}{2y}e^{-(x+y)t} - \frac{(x-y) - d_1}{2y}e^{-(x-y)t}, \qquad (34)$$

where $x = (d_1 + d_2)/2$, $y = \sqrt{(d_1 - d_2)^2 + 4f_1 f_2}/2$, $T_1 = D_1^2/2$, and $T_2 = D_2^2/2$.

Fig. 3 illustrates the properties of the system on the different timescales. The parameters are chosen as follows: $m_1 = m_2 = n_1 = n_2 = 1$, $v = 0$, and $u = 0, 0.5, 1.0, 1.5, 2.0$. Because we set $v = 0$, the only interaction of the two species is $A \rightarrow A + B$, i.e., A can generate B. From the diagram, it is clear that when there is no interaction, the effective temperature is a constant, which means that the fluctuation-dissipation theorem holds. However when there is an interaction, the curves are not straight lines, but instead bend

to the left. The larger the coupling, the more the curve deviates from the straight line. These curves indicate that the fluctuation-dissipation theorem is breaking down in a frequency-dependent way.

A specific two-species example: set thermal rules, then it tends to equilibrium

Here we study a special case to illustrate that the effective temperature in some ways can still play the same role as temperature does in thermodynamics. The interactions are chosen as $u = v$, $m_1 = m_2 = 0$, and $n_1 = n_2 = 1$, i.e., $A \rightarrow B$ and $B \rightarrow A$. This means that A reacts to become B and B reacts to become A.
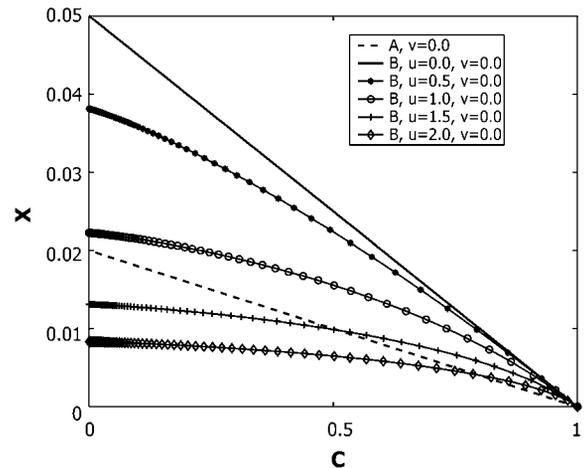

FIGURE 3 Illustration of multiple timescales properties of effective temperature: x axis is the scaled correlation, y axis is the susceptibility. The dashed line represents A, the solid lines with symbols are for B. The solid lines with symbols from up to down correspond to the coupling strengths $u = 0, 0.5, 1.0, 1.5$, and 2.0. The parameters are chosen as following: $k_{g1} = 50.0$, $k_{d1} = 1.0$, $k_{g2} = 20.0$, $k_{d2} = 1.0$, $m_1 = m_2 = n_1 = n_2 = 1$, and $v = 0$.

To investigate the thermalization of the system, we focus on the difference of the two effective temperatures, i.e.

$$\Delta T_{\text{eff}}(\omega) = T_{\text{eff}}^{\text{AA}}(\omega) - T_{\text{eff}}^{\text{BB}}(\omega). \tag{35}$$

Together with Eqs. 29 and 30, the above equation tells us that as the coupling strength increases, the difference between the two effective temperatures decreases. That is, the two temperatures tend to equalize, as the ''hotter'' one drops in temperature and the ''cooler'' one increases in temperature.

Both Figs. 4 and 5 demonstrate this behavior. In Fig. 4, we assumed that the fluctuating terms are uncorrelated and their noise intensities are constant; that is, the terms D_3^{a}, D_3^{b}, D_4^{a}, and D_4^{b} are zero and D_1 and D_2 are constants. The left panel shows that the ''hotter'' species decreases in temperature and the ''cooler'' species increases in temperature monotonically with the increase of their interaction strength. When the coupling is strong enough, the two temperatures converge to the same value. The right panel clearly shows that the difference of the two temperatures decreases with increasing interaction strength.

Fig. 5 shows the result for the general correlated case. In the left panel, we see that both of the temperatures increase at first and then drop after reaching a maximum, and ultimately they converge to the same value. The nonmonotonic behavior, which is different from the uncorrelated case, comes from the correlation of the noise. The curves are similar to stochastic resonance curves (29). Nevertheless, the difference of the two temperatures decreases monotonically, as seen in the right panel.

This example shows that the effective temperature in stochastic kinetics behaves much like ordinary temperature.

REMARKS

The coupling between the two species as well as their own generation and degradation rates determine the effective temperatures. The effective temperatures are thus not always equal, but instead their discrepancy is system- and interaction-dependent. The effective temperature characterizes the properties and the state of that system. For example, with the physically meaningful coupling of the above example,

the system holds the thermal properties: a), the flow goes from ''high'' temperature to ''low'' temperature, and b), if the coupling is strong enough, the temperatures of the two subsystems equalize.

The strategy for calculating effective temperature in solving Eqs. 20 and 21 is quite general, and it can be used to study more complex interaction networks involving multiple species, such as cascades.

EFFECTIVE TEMPERATURE IN GENE NETWORKS

It was suggested that the noise in gene networks can be broken down into intrinsic and extrinsic components (7). If we consider the fluctuations of one particular species of a multiple species interacting network, then intrinsic noise originates from the stochastic nature of the reactions leading to expression of this species alone, whereas extrinsic variability arises from sources that effect the expression of all species. Although this manner of noise classification is useful, it does have some limitations. For example, when there exists a correlation between the noise terms of the different species in a network, as there often is in gene networks, there is no simple way to separate the total noise into intrinsic and extrinsic components.

Fundamentally, the intrinsic-extrinsic classification is actually just the inverse Fourier transform of the power spectrum of the correlation functions, because the noise intensity is just the autocorrelation function of the species. But the power spectrum is more general. For the two species case, Eqs. 25 and 26 give the noise classification expressions. As seen from the expressions, there exist cross-correlation terms between intrinsic sources and extrinsic sources. The power spectrum expressions Eqs. 25 and 26, beyond the intrinsic-extrinsic classification, include the correlated noise sources.

Based on what we know about effective temperature, it appears to be a good candidate for the quantitative analysis of gene networks. To explore this possibility, we will calculate the effective temperature of an unregulated gene present in many copies, and investigate what the effective temperature can tell us about this system.

We assume that there are N copies of a particular gene. Also, assuming that there are x number of bound operators,
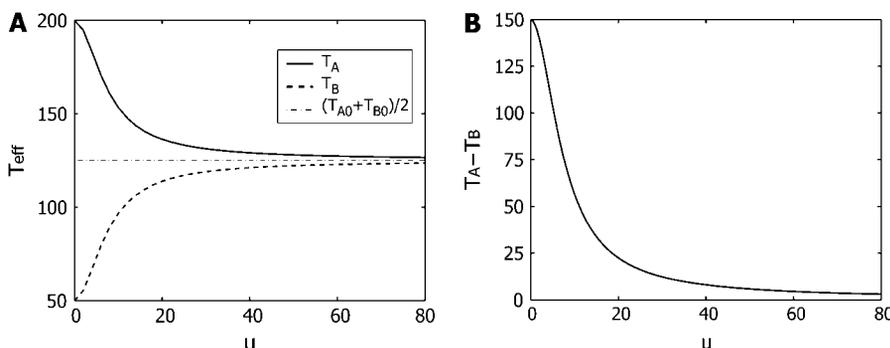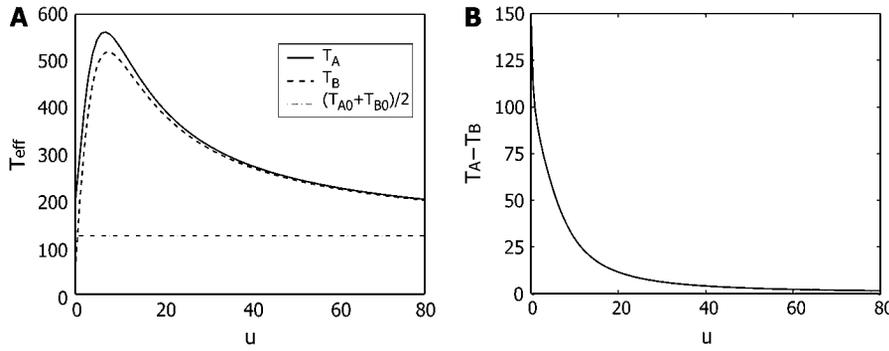

FIGURE 4 Effective temperature versus interaction strength for the noninteracting case. (*Left panel*) The solid line, dashed line, and dash-dotted line stand for the effective temperature of the species A, the effective temperature of the species B, and the mean of the two effective temperatures when there is no coupling. (*Right panel*) The difference of the two effective temperatures in the left panel versus the interaction strength. Here $k_{\text{g1}} = 200.0$, $k_{\text{d1}} = 1.0$, $k_{\text{g2}} = 50.0$, $k_{\text{d2}} = 1.0$, $m_1 = m_2 = 0$, $n_1 = n_2 = 1$, $u = v$, and $w = 10.0$.

FIGURE 5 Effective temperature versus interaction strength for the interacting case. (*Left panel*) The solid line, dashed line, and dash-dotted line stand for the effective temperature of the species A, the effective temperature of the species B, and the mean of the two effective temperatures when there is no coupling. (*Right panel*) The difference of the two effective temperatures in the left panel versus the interaction strength. Here $k_{g1} = 200.0$, $k_{d1} = 1.0$, $k_{g2} = 50.0$, $k_{d2} = 1.0$, $m_1 = m_2 = 0$, $n_1 = n_2 = 1$, $u = v$, and $w = 10.0$.

then the number of unbound operators is $N - x$. The operator sites are assumed to have no explicit regulation (i.e., the operator sites are fluctuating stochastically), and the state of each operator site (bound or unbound) will effect the rate of transcription. k_f and k_b are the binding and unbinding reaction rates for the operator, k_{g1} and k_{g2} are the protein generation rates of a bound operator and an unbound operator, and k_d is the degradation rate of the protein. Given these parameters, the Langevin equations describing the operators and the protein quantity, p, are

$$\frac{dx}{dt} = -k_f x + k_b R_0(N - x) - D_1 \eta_1(t) + D_2 \eta_2(t) \quad (36)$$

$$\frac{dp}{dt} = k_{g1}x + k_{g2}(N - x) - k_d p + D_3 \eta_3(t)$$
$$+ D_4 \eta_4(t) - D_5 \eta_5(t). \quad (37)$$

The noise intensity terms are $D_1 = \sqrt{k_f x}$, $D_2 = \sqrt{k_b R_0(N - x)}$, $D_3 = \sqrt{k_{g1}x}$, $D_4 = \sqrt{k_{g2}x}$, and $D_5 = \sqrt{k_d p}$. The noise $\eta_i(t)$ ($i = 1,2,3,4,5$) is uncorrelated normal Gaussian noise.

From the exact solutions Eqs. 29 and 30 of the general equations Eqs. 20 and 21, we find two different effective temperatures for the DNA and the protein number:

$$T_O(\omega) = T_1 \quad (38)$$

$$T_P(\omega) = T_2 + T_1 \frac{(k_{g1} - k_{g2})^2}{\omega^2 + (k_f + k_b)^2}. \quad (39)$$

Here $T_1 = D_1^2 + D_2^2$ and $T_2 = D_3^2 + D_4^2 + D_5^2$ with the substitutions of x and p by the steady-state values x^* and y^*. T_1 and T_2 are independent on the frequency.

These results show that the effective temperature of the DNA $T_O(\omega)$, T_1 is independent of the protein. The effective temperature of the protein $T_P(\omega)$, on the other hand, is composed of two parts, T_2 and $T_1(k_{g1} - k_{g2})^2/(\omega^2 + (k_f + k_b)^2)$, which means that the "hotness" of the DNA actually effects the temperature of the protein. This is logical since the operator sites regulate the downstream production of the protein, but the protein does not regulate the production of the DNA.

To relate this to the notion of intrinsic and extrinsic noise, we can study the proteins as our system. Using this system,

the fluctuation of the proteins due to the stochasticity of the chemical reaction Eq. 37 is the intrinsic noise, whereas the fluctuation of the DNA operator is the extrinsic noise. Using a standard method to calculate the total noise (7,11), we may write the total noise for this unregulated gene system in terms of intrinsic and extrinsic noises as

$$\sigma_t^2 = \sigma_{in}^2 + \sigma_{ex}^2. \quad (40)$$

Following the same strategy that we used in the study of a two-species process, the equivalent power spectrum expression is

$$C_p(\omega) = \frac{D_3^2 + D_4^2 + D_5^2}{k_d^2 + \omega^2} + \frac{(k_{g1} - k_{g2})^2(D_1^2 + D_1^2)}{[(k_f + k_b)^2 + \omega^2](k_d^2 + \omega^2)}$$
$$= \frac{1}{k_d^2 + \omega^2} \cdot T_2 + \frac{(k_{g1} - k_{g2})^2}{[(k_f + k_b)^2 + \omega^2](k_d^2 + \omega^2)} \cdot T_1 \quad (41)$$

Comparing the power spectrum expression with the effective temperature Eq. 39, we see that the effective temperature can function as an alternative means to quantify and analyze different sources of noise in gene networks. In this example, the temperature T_P divides noise into intrinsic and extrinsic components, but separates the noise source via timescale. In addition, because the effective temperature can measure the stability of a system (17), here T_{eff}^P tells how much of effective temperature (T_2) comes from the intrinsic noise (σ_{in}^2) and how much of the effective temperature ($T_1(k_{g1} - k_{g2})^2/(\omega^2 + (k_f + k_b)^2)$) comes from the extrinsic noise (σ_{ex}^2). This gives a measure of the contributions of intrinsic and extrinsic noises to the "hotness" of the system, which is not merely a summation of intrinsic and extrinsic noise components. Moreover, the effective temperature explores the frequency selectivity of the system. From the expression of the effective temperature Eq. 39, we can see that the intrinsic noise always contributes to the system, but the extrinsic noise is frequency dependent. We see that the extrinsic noise plays an important role in the low frequency region, but it is filtered out in the high frequency region. This underlying property is masked by the power spectrum expression, demonstrating an advantage of using the effective temperature.

CONCLUSIONS AND DISCUSSIONS

Temperature is a central notion of thermodynamics, and the fluctuation-dissipation theorem is important in near equilibrium statistical mechanics. However, the theorem breaks down for stochastic dynamical kinetics and gene networks since such systems are far from equilibrium. The FD plot introduced in glass theory nevertheless provides an understanding of the interacting stochastic processes.

The effective temperature in general is observable dependent and therefore is not unique, but when the systems are large, it has some of the same valuable properties as found when describing glasses (14). The observable-dependence shows that a birth-death process in a steady state is nevertheless not an equilibrium system. Although there are multiple effective temperatures corresponding to different types of correlations, the properly chosen effective temperature can be used to explore the dynamic properties of a system. The autocorrelation effective temperature in a simple situation controls the flow between two interacting biochemical species.

Effective temperature provides an alternative language for discussing the origin of noises in stochastic cell biology. It goes beyond the intrinsic-extrinsic classification that has already been introduced and works in cases where the noise of various species is correlated.

Moreover, using the general definition of the effective temperature for out-of-equilibrium systems, it should also be applicable to more complex genetic circuits that do not relax to fixed steady states, such as repressor oscillators (30). When spatial heterogeneities in real cells are considered, diffusion and transportation of regulatory proteins also can have a great impact (31). The slowness of the ordered dynamics of the regulatory networks in comparison to the molecular events suggests that the idea of effective temperature could be generally useful. Further developments of the concept of effective temperature as a means to characterize more complex gene networks will be needed, however, to increase our understanding of multi-gene regulation in organisms.

APPENDIX A: THE CALCULATION OF CORRELATION AND RESPONSE FUNCTIONS FOR A BIRTH-DEATH PROCESS

To calculate the correlation and response functions, we need an expression for the time-dependent observables in Heisenberg representation. From Eqs. 14 and 17, we find that the expressions of $\hat{a}^+(t)$ and $\hat{a}(t)$ are sufficient to describe the birth-death process.

The non-Hermitian time-dependent expression of $\hat{a}$ is

$$\hat{a}^+(t) \equiv e^{-\hat{L}t} \cdot \hat{a}^+ \cdot e^{\hat{L}t} \tag{42}$$

with the Lagrangian of the system $\hat{L} = k_g(\hat{a}^+ - 1) + k_d(\hat{a} - \hat{a}^+\hat{a})$.

To do this we use the following identity:

$$e^{x\hat{A}}\hat{B}e^{-x\hat{A}} = \hat{B} + \frac{x}{1!}[\hat{A}, \hat{B}] + \frac{x^2}{2!}[\hat{A}, [\hat{A}, \hat{B}]]$$
$$+ \frac{x^3}{3!}[\hat{A}, [\hat{A}, [\hat{A}, \hat{B}]]] + \cdots \tag{43}$$

The algebra of the operators is given as

$$\hat{a}^+ = \hat{a}^+$$
$$[\hat{L}, \hat{a}^+] = k_d(1 - \hat{a}^+)$$
$$[\hat{L}, [\hat{L}, \hat{a}^+]] = -k_d^2(1 - \hat{a}^+)$$
$$[\hat{A}, [\hat{A}, [\hat{A}, \hat{B}]]] = k_d^3(1 - \hat{a}^+)$$
$$\cdots$$

Summarizing all of the above terms yields the expression for $\hat{a}^+(t)$:

$$\hat{a}^+(t) = \hat{a}^+ + \frac{-1}{1!}k_d(1 - \hat{a}^+) - \frac{1}{2!}k_d^2(1 - \hat{a}^+)$$
$$+ \frac{-1}{3!}k_d^3(1 - \hat{a}^+) + \cdots$$
$$= (\hat{a}^+ - 1)e^{k_d t} + 1 \tag{44}$$

Similarly, we have an expression for $\hat{a}(t)$:

$$\hat{a}(t) \equiv e^{-\hat{L}t} \cdot \hat{a} \cdot e^{\hat{L}t} = \left(\hat{a} - \frac{k_g}{k_d}\right)e^{-k_d t} + \frac{k_g}{k_d} \tag{45}$$

Now we can calculate the correlation and response functions. For a perturbation of generation rate $k_g \rightarrow k_g + h(t)$, the Lagrangian $\hat{L}$ is perturbed by a small term $-h(t)(\hat{a}^+ - 1)$. Using the time-dependent expressions of $\hat{a}(t)$ and $\hat{a}(t)^+$, we have the correlation and response functions:

$$C(t', t) = \langle \hat{a}^+(t')\hat{a}(t')\hat{a}^+(t)\hat{a}(t)\rangle$$
$$= \langle 0|e^{\hat{a}} \cdot \hat{a}^+(t')\hat{a}(t')\hat{a}^+(t)\hat{a}(t) \cdot e^{\frac{k_g}{k_d}(\hat{a}^+ - 1)}|0\rangle$$
$$= u_s^2 + u_s e^{-k_d(t'-t)} \tag{46}$$

$$R(t', t) \equiv \frac{\delta\langle \hat{a}^+(t')\hat{a}(t')\rangle}{\delta h(t)}$$
$$= \langle 0|e^{\hat{a}} \cdot [\hat{a}^+(t')\hat{a}(t')(\hat{a}^+(t) - 1)$$
$$- (\hat{a}^+(t') - 1)\hat{a}^+(t)\hat{a}(t)] \cdot e^{\frac{k_g}{k_d}(\hat{a}^+ - 1)}|0\rangle$$
$$= e^{-k_d(t'-t)}. \tag{47}$$

The corresponding effective temperature is derived from the definition Eq. 5:

$$T_{eff}(\omega) \equiv \frac{\omega \tilde{C}'_{12}(\omega)}{\tilde{R}''_{12}(\omega)} = \frac{-\partial_t C(t', t)}{R(t', t)} = k_g. \tag{48}$$

For a perturbation of degradation rate, the Liouvillian is perturbed by a small term $-h(t)(\hat{a} - \hat{a}^+\hat{a})$. The correlation and response functions are

$$C(t', t) = \frac{1}{2}\langle \hat{a}^+(t')\hat{a}(t')\hat{a}^+(t)\hat{a}(t)\hat{a}^+(t)\hat{a}(t)\rangle$$
$$= \frac{1}{2}\langle 0|e^{\hat{a}} \cdot \hat{a}^+(t')\hat{a}(t')\hat{a}^+(t)\hat{a}(t)\hat{a}^+(t)\hat{a}(t) \cdot e^{\frac{k_g}{k_d}(\hat{a}^+ - 1)}|0\rangle$$
$$= \frac{1}{2}(u_s^3 + u_s^2 + 2u_s^2 e^{-k_d(t'-t)} + u_s e^{-k_d(t'-t)}) \tag{49}$$

$$R(t', t) \equiv \frac{\delta \langle \hat{a}^+(t') \hat{a}(t') \rangle}{\delta h(t)}$$

$$= \langle 0 | e^{\hat{a}} \cdot \hat{a}^+(t') \hat{a}(t') [\hat{a}(t) - \hat{a}^+(t) \hat{a}(t)]$$

$$- [\hat{a}(t') - \hat{a}^+(t') \hat{a}(t')] \hat{a}^+(t) \hat{a}(t) \cdot e^{\frac{k_g}{k_d}(\hat{a}^+ - 1)} | 0 \rangle$$

$$= u_s e^{-k_d(t'-t)} \qquad (50)$$

from which the effective temperature can be derived:

$$T_{eff}(\omega) \equiv \frac{\omega \tilde{C}'_{12}(\omega)}{\tilde{R}''_{12}(\omega)} = \frac{-\partial_t C(t', t)}{R(t', t)} = k_g + \frac{1}{2} k_d \qquad (51)$$

APPENDIX B: SOLVING EQS. 20 AND 21

By taking the Fourier transform of Eqs. 20 and 21, we have

$$(d_1 - i\omega)\tilde{A}(\omega) - f_2 \tilde{B}(\omega) = D_1 \tilde{\xi}_1(\omega) + D_3^a \tilde{\xi}_3(\omega)$$
$$+ D_4^a \tilde{\xi}_4(\omega) + k_{g1}\delta(\omega) \qquad (52)$$

$$-f_1 \tilde{A}(\omega) + (d_2 - i\omega)\tilde{B}(\omega) = D_2 \tilde{\xi}_2(\omega) + D_3^b \tilde{\xi}_3(\omega)$$
$$+ D_4^b \tilde{\xi}_4(\omega) + k_{g2}\delta(\omega), \qquad (53)$$

where the noise intensities D_1, D_2, D_3^a, D_3^b, D_4^a, and D_4^b depend only on the steady-state values A^* and B^* of the two species.

These two equations can be solved as

where the delta functions are ignored since they have no contribution in the

$$(d_1 - i\omega)\tilde{A}(\omega) - f_2 \tilde{B}(\omega) = D_1 \tilde{\xi}_1(\omega) + D_3^a \tilde{\xi}_3(\omega) + D_4^a \tilde{\xi}_4(\omega)$$
$$+ \tilde{h}_1(\omega) + k_{g1}\delta(\omega) \qquad (58)$$

$$-f_1 \tilde{A}(\omega) + (d_2 - i\omega)\tilde{B}(\omega) = D_2 \tilde{\xi}_2(\omega) + D_3^b \tilde{\xi}_3(\omega) + D_4^b \tilde{\xi}_4(\omega)$$
$$+ \tilde{h}_2(\omega) + k_{g2}\tilde{\xi}(\omega) \qquad (59)$$

from which the response functions can be derived:

$$R_{AA} = \frac{\delta \langle \tilde{A}(\omega) \rangle}{\delta \tilde{h}_1(\omega)} = \frac{i\omega - d_2}{\omega^2 + i\omega(d_1 + d_2) + f_1 f_2 - d_1 d_2} \qquad (61)$$

$$R_{BB} = \frac{\delta \langle \tilde{B}(\omega) \rangle}{\delta \tilde{h}_2(\omega)} = \frac{i\omega - d_1}{\omega^2 + i\omega(d_1 + d_2) + f_1 f_2 - d_1 d_2}. \qquad (62)$$

REFERENCES

1. McAdams, H., and A. Arkin. 1999. It's a noisy business! Genetic regulations at nanomolar scale. *Trends Genet.* 15:65–69.

later calculations of correlation and response functions.

The autocorrelation functions for the species A and B are thus

To calculate the response functions, we introduce two small perturbations $\tilde{h}_1(\omega)$ and $\tilde{h}_1(\omega)$ to the system:

$$\tilde{A}(\omega) = \frac{D_1(d_2 - i\omega)\tilde{\xi}_1(\omega) + D_2 f_2 \tilde{\xi}_2(\omega) + [D_3^a(d_2 - i\omega) + D_3^b f_2]\tilde{\xi}_3(\omega) + [D_4^a(d_2 - i\omega) + D_4^b f_2]\tilde{\xi}_4(\omega)}{\omega^2 - i\omega(d_1 + d_2) + f_1 f_2 - d_1 d_2} \qquad (54)$$

$$\tilde{B}(\omega) = \frac{D_1 f_1 \tilde{\xi}_1(\omega) + D_2(d_1 - i\omega)\tilde{\xi}_2(\omega) + [D_3^a f_1 + D_3^b(d_1 - i\omega)]\tilde{\xi}_3(\omega) + [D_4^a f_1 + D_4^b(d_1 - i\omega)]\tilde{\xi}_4(\omega)}{\omega^2 - i\omega(d_1 + d_2) + f_1 f_2 - d_1 d_2}, \qquad (55)$$

$$C_{AA} = \frac{(\omega^2 + d_2^2)D_1^2 + f_2^2 D_2^2 + [(d_2 D_3^a + f_2 D_3^b)^2 + \omega^2(D_3^a)^2] + [(d_2 D_4^a + f_2 D_4^b)^2 + \omega^2(D_4^a)^2]}{(\omega^2 + f_1 f_2 - d_1 d_2)^2 + (d_1 + d_2)^2 \omega^2} \qquad (56)$$

$$C_{BB} = \frac{f_1^2 D_1^2 + (\omega^2 + d_1^2)D_2^2 + [(f_1 D_3^a + d_1 D_3^b)^2 + \omega^2(D_3^b)^2] + [(f_1 D_4^a + d_1 D_4^b)^2 + \omega^2(D_4^b)^2]}{(\omega^2 + f_1 f_2 - d_1 d_2)^2 + (d_1 + d_2)^2 \omega^2}. \qquad (57)$$

2. Kaern, M., W. J. Blake, and J. J. Collins. 2003. The engineering of gene regulatory networks. *Annu. Rev. Biomed. Eng.* 5:179–206.

3. Hasty, J., D. McMillen, and J. Collins. 2002. Engineered gene circuits. *Nature.* 420:224–230.

4. Gillespie, D. T. 1977. Exact stochastic simulation of coupled chemical reactions. *J. Phys. Chem.* 81:2340–2361.

5. Rao, C. V., and A. P. Arkin. 2003. Stochastic chemical kinetics and the quasisteady-state assumption: application to the Gillespie algorithm. *J. Chem. Phys.* 118:4999–5010.

6. Lu, T., D. Volfson, L. Tsimring, and J. Hasty. 2004. Cellular growth and division in the Gillespie algorithm. *IEE Systems Biology.* 1:121–127.

7. Swain, P., M. Elowitz, and E. Siggia. 2002. Intrinsic and extrinsic contributions to stochasticity in gene expression. *Proc. Natl. Acad. Sci. USA.* 99:12795–12800.

8. Thattai, M., and A. van Oudenaarden. 2001. Intrinsic noise in gene regulatory networks. *Proc. Natl. Acad. Sci. USA.* 98:8614–8619.

9. Pedraza, J., and A. Van Oudenaarden. 2005. Noise propagation in gene networks. *Science.* 307:1965–1969.

10. Paulsson, J. 2004. Summing up the noise in gene networks. *Nature.* 427:415–418.

11. Shibata, T., and K. Fujimoto. 2005. Noisy signal amplification in ultrasensitive signal transduction. *Proc. Natl. Acad. Sci. USA.* 102:331–336.

12. Kubo, R. 1966. The fluctuation-dissipation theorem. *Rep. Prog. Phys.* 29:255–284.

13. Halliday, D., R. Resnick, and J. Walker. 1997. Fundamentals of Physics, 5th ed. John Wiley & Sons, New York.

14. Kurchan, J. 2005. In and out of equilibrium. *Nature.* 433:222–225.

15. Cugliandolo, L., J. Kurchan, and L. Peliti. 1997. Energy flow, partial equilibration and effect temp in systems with slow dynamics. *Phys. Rev. E.* 55:3898–3914.

16. Cugliandolo, L., and J. Kurchan. 1999. Thermal properties of slow dynamics. *Physica A.* 263:242–251.

17. Shen, T., and P. G. Wolynes. 2004. Stability and dynamics of crystals and glasses of motorized particles. *Proc. Natl. Acad. Sci. USA.* 101:8547–8550.

18. Martin, P., A. Hudspeth, and F. Julicher. 2001. Comparison of a hair bundle's spontaneous oscillations with its response to mechanical stimulation reveals the underlying active process. *Proc. Natl. Acad. Sci. USA.* 98:14380–14385.

19. Einstein, A. 1905. On the movement of small particles suspended in stationary liquids required by the molecular-kinetic theory of heat. *Ann. Phys. Lpz.* 17:549–560.

20. Bialek, W. 2000. Stability and noise in biochemical switches. arxiv.org/abs/cond-mat/0005235.

21. Mattis, D., and M. Glasser. 1998. The uses of quantum field theory in diffusion-limited reactions. *Phys. Rev. E.* 70:979–1001.

22. Eyink, G. 1996. Action principle in nonequilibrium statistical dynamics. *Phys. Rev. E.* 54:3419–3435.

23. McQuarrie, D. 1967. Stochastic Approach to Chemical Kinetics. Methuen & Co., London.

24. Dattoli, G., A. Torre, and R. Mignani. 1990. Non-Hermitian evolution of two-level quantum systems. *Phys. Rev. A.* 42:1467–1475.

25. Bakk, A., and R. Metzler. 2004. Nonspecific binding of the O_R repressors CI and Cro of bacteriophage λ. *J. Theor. Biol.* 231:525–533.

26. Bakk, A., R. Metzler, and K. Sneppen. 2004. Sensitivity of phage lambda upon variations of the Gibbs free energy. *Isr. J. Chem.* 44:309–315.

27. Metzler, R., and P. G. Wolynes. 2002. Number fluctuations and the threshold model of kinetic switches. *Chem. Phys.* 284:469–479.

28. Gillespie, D. 2000. The chemical Langevin equation. *J. Chem. Phys.* 113:297–306.

29. Gammaitoni, L., P. Hangi, P. Jung, and F. Marchesoni. 1998. Stochastic resonance. *Rev. Mod. Phys.* 70:223–287.

30. Elowitz, M. B., and S. Leibler. 2000. A synthetic oscillatory network of transcriptional regulators. *Nature.* 403:335–338.

31. Metzler, R., and J. Klafter. 2004. The restaurant at the end of the random walk: recent developments in the description of anomalous transport by fractional dynamics. *J. Phys. A.* 37:R161–R208.